RSC Advances

ROYAL SOCIETY OF CHEMISTRY

www.rsc.org/advances

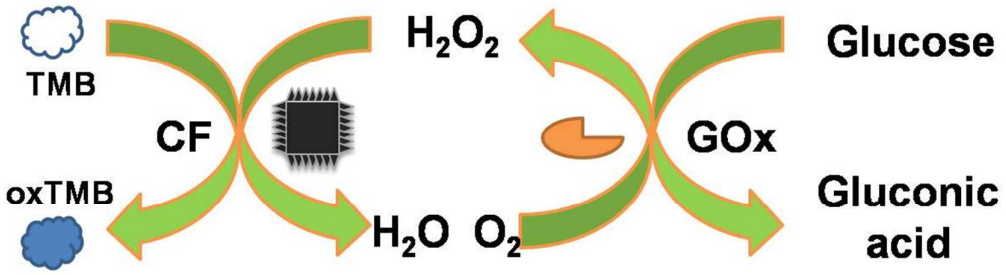

A facile approach was proposed for the synthesis of hierarchical $Co_xFe_{3-x}O_4$ (CF) nanocubes, using Prussian Blue (PB) as precursor. Then, an efficient and simple colorimetric biosensor for H_2O_2 and glucose was fabricated using CF nanocubes as peroxidase mimetic.

Cite this: DOI: 10.1039/c0xx00000x

www.rsc.org/xxxxxx

ARTICLE TYPE

$Co_xFe_{3-x}O_4$ hierarchical nanocubes as peroxidase mimetics and their applications in H_2O_2 and glucose detection

Wenshu Yang[a,b], Jinhui Hao[a,b], Zhe Zhang[a], Baoping Lu[a,b], Bailin Zhang[*a] and Jilin Tang[*a]

Received (in XXX, XXX) Xth XXXXXXXXX 20XX, Accepted Xth XXXXXXXXX 20XX
DOI: 10.1039/b000000x

A facile approach was proposed for the synthesis of hierarchical $Co_xFe_{3-x}O_4$ nanocubes (CF nanocubes), using Prussian Blue (PB) as precursor. The method consists of the synthesis of hierarchical cobalt-iron Prussian blue analogue (PBA) through the reaction of PB nanocubes with $CoCl_2$ under water bath and subsequently calcining the corresponding PBA precursor. The obtained CF nanocubes were characterized using transmission electron microscopy, scanning electron microscopy, X-ray diffraction, X-ray photoelectron spectroscopy and N_2 adsorption-desorption isotherm measurements. It is found that the hierarchical CF nanocubes have a large specific surface area (108 $m^2 g^{-1}$). Considering the hierarchical structure and the doping of Co in Fe_3O_4 are beneficial for the catalytic activity of catalyst, an efficient and simple colorimetric biosensor for H_2O_2 and glucose was fabricated using CF nanocubes as peroxidase mimetic. The good catalytic activity and low-cost make the hierarchical CF nanocubes a useful biocatalyst for a wide range of potential applications in medicine and biotechnology.

Introduction

In recent years, peroxidase, which is common in nature and could be used for hydrogen peroxide (H_2O_2) detection, has played an important role for a variety of practical applications [1, 2]. However, such natural enzymes bear some serious drawbacks in that they are unstable against denaturation or protease digestion [3]. While the artificial enzyme mimetics have some advantages including well resistance to extremes reaction conditions and low cost, this could overcome these limitations [4]. Therefore, lots of efforts have been made to use stable enzyme mimetics as substitutes for natural enzymes. For example, a variety of peroxidase-like nanomaterials such as noble metal [5], graphene [6] and graphene-based materials [7-9], Fe_3O_4 and its substituted ferrite [10-13] have been extensively used as enzyme mimetics for detection of H_2O_2. $Co_xFe_{3-x}O_4$ ferrite is a kind of single-phase mixed metal oxides with Co and Fe cations. The structure of $Co_xFe_{3-x}O_4$ transforms from normal spinel into inverse spinel as x decreases that leads to the appearance of new active sites in the samples [14, 15]. It is known that $Co_xFe_{3-x}O_4$ can catalyze the reduction of H_2O_2 at low concentration with remarkable sensitivity [10, 16, 17]. The high catalytic activity and low-cost have made $Co_xFe_{3-x}O_4$ to be one of the most promising candidates as peroxidase mimetics.

Compared to traditional materials, the high-surface-area of materials is not only dependent on their bulk, but also their structures on the nanoscale. Among various nanostructures, hierarchical materials have the merit of high surface-to-bulk ratio, which can provide more reaction active sites [18-21]. The peroxidase mimetics catalytic performance of Co-doping catalysts could be improved by constructing a hierarchical nanostructure. It is desirable to develop a method for the fabrication of $Co_xFe_{3-x}O_4$ with well-defined hierarchical structures. Up to now, many nanostructures of $Co_xFe_{3-x}O_4$ have been fabricated such as nanospheres [22], nanoparticles [23, 24], nanorods [25] and nanotubes [26]. To the best of our knowledge, there is no report about the synthesis of hierarchical $Co_xFe_{3-x}O_4$ nanocubes and investigation them as peroxidase mimetics. In this paper, a kind of hierarchical cobalt iron oxide (CF) nanocubes was synthesized by using Prussian Blue (PB) as precursor. As depicted in Scheme 1, PB nanocubes were firstly mixed with a cobalt chloride solution. After water bath treatment at 80 °C, the PB nanocubes were converted to hierarchical nanostructured cobalt-iron Prussian blue analogue (PBA). In the second step, hierarchical PBA nanocubes were transformed into CF nanocubes by calcinations, and the hierarchical morphology was still retained. It is found that the hierarchical nanostructured CF nanocubes possess excellent intrinsic peroxidase-like activity for detection of H_2O_2 and glucose. These display the promising future of hierarchical CF nanocubes as enzyme mimics to construct biosensors.

Experiment

Materials and Apparatus

Poly (*N*-vinyl-2-pyrrolidone) (PVP, relative molecular mass 30,000–40,000) was obtained from Shanghai Chemical Factory (Shanghai, China). 3,3',5,5'-Tetramethylbenzidine (TMB) and glucose oxidase (GOx) were obtained from Aladdin (Shanghai, China). Glucose, H_2O_2, $K_4Fe(CN)_6 \cdot 3H_2O$, $CoCl_2 \cdot 6H_2O$ and urea were purchased from Beijing Chemical Reagent Factory (Beijing, China). The serum samples were provided by Northeast Normal

University Hospital. Other reagents were of analytical grade and were used as received. All aqueous solutions were prepared with Milli-Q water (≥18.2 MΩ·cm) from a Milli-Q Plus system (Millipore).

UV–Vis detection was carried out on a Cary 500 UV–Vis–NIR spectrophotometer (Varian, USA). X-ray photoelectron spectroscopy (XPS) measurements were performed on an ESCALAB MKII spectrometer (VG Co., United Kingdom) with Al Kα X-ray radiation as X-ray source for excitation. Samples for XPS characterization were powders. X-ray diffraction (XRD) spectra were obtained using a D8 ADVANCE diffractometer (Bruker, Germany) using Cu Kα (0.15406 nm) radiation. Scanning electron microscopy (SEM) images and mapping analysis were inspected on a Hitachi S-4800 microscope. Transmission electron microscopy (TEM) images were obtained with a Hitachi H600 electron microscope (Japan) with an accelerating voltage of 100 kV. Samples for SEM and TEM characterizations were prepared by placing a drop of prepared solution on a silicon wafer and a carbon-coated copper grid, respectively, then drying at room temperature. Nitrogen adsorption and desorption isotherms were measured on an ASAP 2020 (Micromeritics, USA). Pore size distribution (PSD) curves were calculated by the Barrett–Joyner–Halenda (BJH) method from the absorption branch.

Synthesis of $Co_xFe_{3-x}O_4$ hierarchical nanocubes

Firstly, PB nanocubes were prepared by a simple method according to the literature [27]. In a typical procedure, PVP (3.8 g) and $K_4Fe(CN)_6·3H_2O$ (0.11 g) were added to a HCl solution (0.1 M, 50 mL) under magnetic stirring. After the mixture was stirred for 30 min, the bottle was then placed into an electric oven and heated at 80 °C for 24 h. The obtained blue product was washed several times with deionsized water and finally dried at room temperature for further use. Secondly, the as-obtained PB nanocubes (1 mg) were diluted with 20 mL Milli-Q water in a glass container and subjected to ultrasound for 10 minutes. Then, 0.01 mmol $CoCl_2·6H_2O$ and 0.6 mmol urea were added and sonicated for 1 min to form a homogeneous solution. The resulting mixture was sealed and maintained at 80 °C for 12 hours. After cooled to room temperature, the product (PBA) was collected and washed with ethanol several times, and dried at 60 °C for 12 hours. Hierarchical CF nanocubes were made by annealing the corresponding PBA precursor at 350 °C in air for 6 h with a slow heating rate of 2 °C min^{-1}.

Detection of H_2O_2 and glucose using CF nanocubes as peroxidase mimetics

For detection of H_2O_2, experiments were carried out using 20 μg CF nanocubes in a reaction volume of 2 mL NaAc-HAc buffer (pH 4.0) with 500 μM TMB as substrate. The concentration of H_2O_2 was 50 mM, unless otherwise stated. Reactions were monitored at 652 nm and recorded after 10 min at 40℃.

The determination of glucose was performed as follow: firstly, 10μL of GOx (10 mg/mL) and 190 μL of glucose with different concentrations in PBS buffer (0.01mM, pH 7.4) were incubated at 37 °C for 0.5 h; then 100μL of TMB (5mM, ethanol solution), 690 μL of NaAc-HAc buffer (0.1 M, pH 4.0), and 10 μL of CF nanocubes catalyst (1mg/mL) were added into the above 200 μL reaction solution; finally, the mixed solution was incubated at 40°C for 10 min for absorbance measurement.

The serum samples firstly centrifuged at 10000 rpm for 10 min. Then the samples were diluted 50 times using PBS buffer (0.01mM, pH 7.4). The glucose detection in serum was measured as described above. For selective experiment, 5 mM lactose, 5 mM maltose, and 5 mM sucrose were used instead of 0.5 mM glucose for the assay.

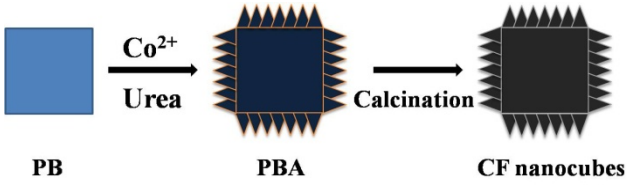

Scheme 1. Illustration of the procedure used to prepare CF nanocubes

Results and Discussion

Characterization of catalysts

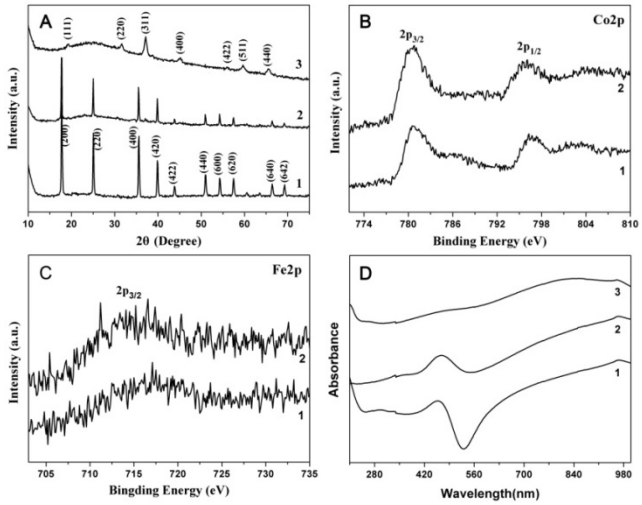

Fig.1 XRD patterns (A) of PB (trace 1), PBA (trace 2) and CF nanocubes (trace 3). XPS spectra of Co2p (B) and Fe2p (C) in PBA (trace1) and CF nanocubes (trace 2). UV-Vis spectra (D) of PB (trace 1), PBA (trace 2) and CF (trace 3) nanocubes.

In this paper, the water bath reaction coupled with post annealing was applied to fabricate hierarchical CF nanocubes. XRD was initially used to verify crystal phases of the as-prepared nanocomposites. Fig. 1A (trace 1) shows the XRD pattern of the synthesized PB nanocubes (JCPD card No.73-0687). It can be seen from Fig. 1A (trace 2), the PB has converted to PBA (JCPD card No.75-0038) with a face-centered cubic structure, after reacting with $CoCl_2$ under water bath. Then the PBA nanocubes were annealed at 350 °C in air. The XRD characteristic peaks of PBA disappeared completely, and some new peaks arising from CF nanocubes were observed (Fig. 1A, trace 3). The XRD peaks of CF shown in Fig. 1A (trace 3) are well matched with the single phase of $Co_xFe_{3-x}O_4$ (JCPDS Card no. 74-3417) with a face-centered cubic spinel structure. In addition, the sharp peaks confirmed that the CF nanocubes were well crystallized.

XPS analysis was performed to investigate the elemental composition of PBA and CF nanocubes. The Co2p spectrum of PBA (Fig. 1B (trace 1)) has two main $2p_{3/2}$ and $2p_{1/2}$ spin−orbit lines at 780.5 eV and 795.7 eV, respectively. No obvious shift of

Co2p spectrum in CF nanocubes is observed after annealing PBA precursor (Fig.1B, trace 2), which indicates that there is no significant change in the oxidation state of cobalt by calcinations. Fig.1C shows the Fe2p spectra of PBA and CF nanocubes. Similarly, calcination also has not resulted in a change in oxidation state of Fe element. The Co-doping level was determined by energy dispersive spectroscopy (EDS) analysis, which showed the atomic ratio of Co/Fe was close to 1/2.5 (Fig. S1). Furthermore, UV–Vis spectra of the as-prepared nanocomposites in water were presented in Fig.1D. No obviously characteristic absorption peak of CF nanocubes (Fig.1D, trace 3) is observed comparing with PB (Fig.1D, trace 1) and PBA (Fig.1D, trace 2), which indicates the formation of new phase.

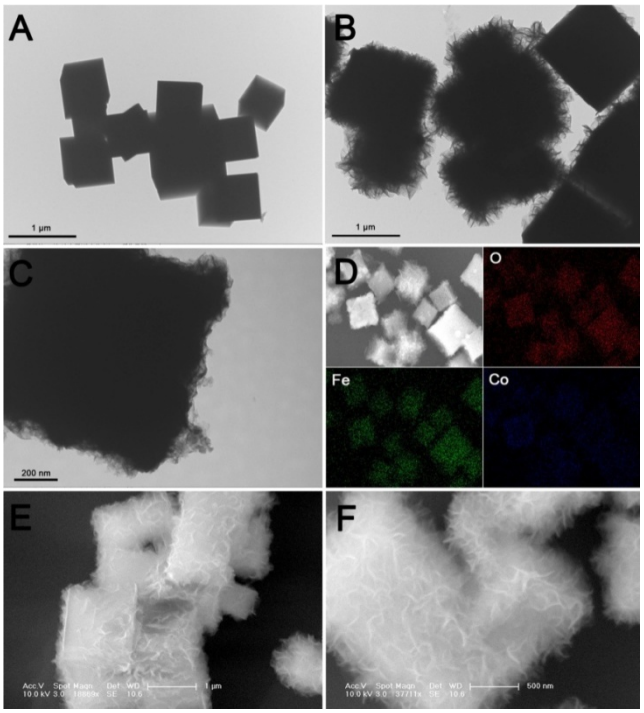

Fig.2 TEM images of PB (A), PBA (B) and CF nanocubes (C). SEM element mapping of CF nanocubes (D). SEM images of PBA (E) and CF nanocubes (F).

The morphologies of the PBA and the calcined CF nanocubes were investigated by SEM and TEM (Fig.2). The PBA (Fig. 2B) obtained by water bath reaction shows a larger cubic structure with the size of ~1μm compared with PB nanocubes (~600 nm) (Fig. 2A). Moreover, the smooth surface of PB (Fig. 2A) apparently changed to hierarchical structure (Fig. 2B) after conversion into PBA. Through calcined process, the hierarchical morphology and size of nanocubes were still remained, although the phase has transformed from PBA to CF nanocubes (Fig. 2B and C). To further substantiate the structure of nanomaterials, SEM studies were performed. After Co^{2+} was doped into PB, it is visibly observed that the nanosheets on the surface of PBA (Fig. 2E) interconnect with each other and form a hierarchical character. Even PBA conversion into CF nanocubes, the hierarchical morphology has not significant alterations. Elemental mapping analysis (Fig. 2D) clearly reveals the uniform distribution of O, Co, and Fe elements within the CF nanocubes.

The surface area and porosity property of hierarchical CF nanocubes were investigated by Brunauer-Emmett-Teller (BET) N_2-adsorption/desorption analysis. The adsorption-desorption exhibits typical type-IV isotherms (Fig. 3), indicating the

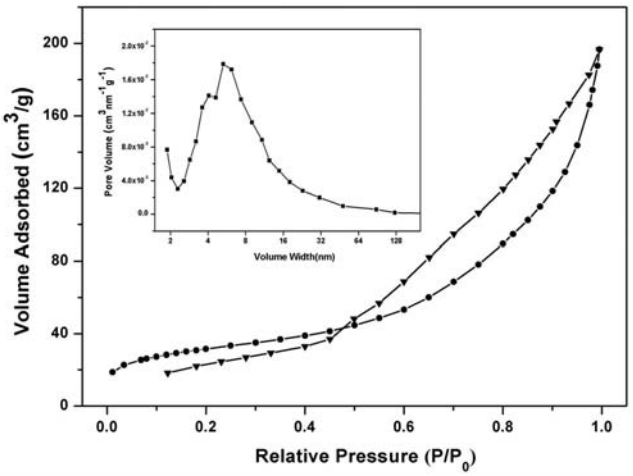

Fig.3 N_2 adsorption−desorption isotherms of CF nanocubes (Inset: BJH pore size distribution).

existence of mesopores microstructure. This result was further confirmed by the BJH pore size distribution plot (inset in Fig. 3), which suggests that the CF nanocubes contain pores with a diameter about 7.48 nm. Importantly, the hierarchical structure of CF nanocubes gave rise to a relatively high BET surface area of 108 $m^2 g^{-1}$, which may be desirable for catalytic reactions.

Detection of H_2O_2 and Glucose

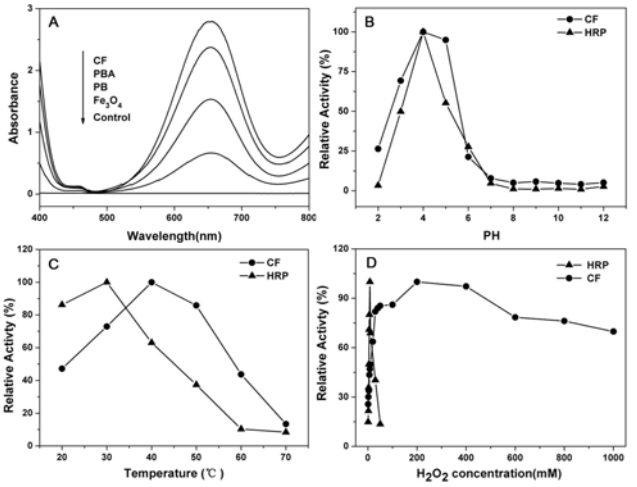

Fig.4 UV-Vis absorption spectra of TMB (500 μM) and H_2O_2 (50mM) reaction solutions in the presence of different catalysts (A).Dependence of the peroxidase-like activity of CF nanocube and HRP on pH (B), temperature (C), and H_2O_2 concentration (D).

Hierarchical nanomaterials with a high specific surface area are usually employed for catalysis due to their capability to provide a large quantity of reactive sites [18, 28, 29]. Moreover，the metal doped Fe_3O_4 nonaparticles have a better catalytic performance compared with pure Fe_3O_4 nonaparticles [11, 30]. Inspired by these ideas, we investigate the application of the obtained hierarchical CF nanocubes as peroxidase mimetics. The catalytic oxidation of TMB was detected by UV-Vis spectroscopy. Fig.S2 shows the UV-Vis spectra of TMB solution in acetate buffer (pH 4.0) under

different conditions. It can be found that TMB solutions in presence of only H_2O_2 or CF nanocubes exhibit no obvious adsorption peaks in the range 400 to 800 nm. However, there is a strong adsorption peak at 652 nm for TMB solution in presence of both H_2O_2 and CF nanocubes, which is attributed to the

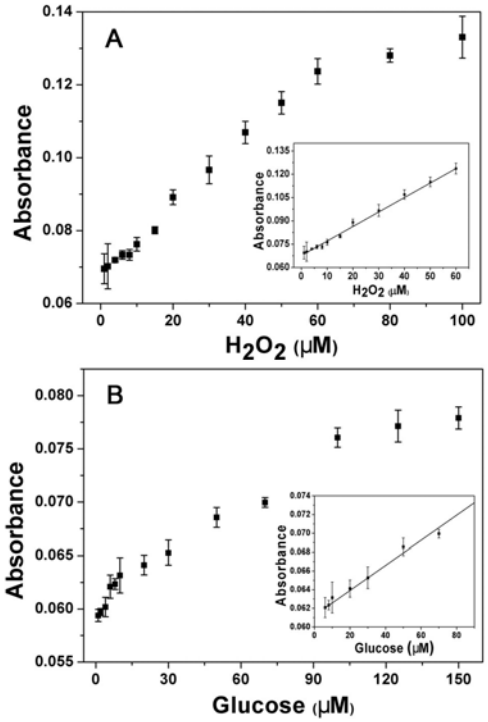

Fig.5 The dose-response curves for H_2O_2 (A) and glucose (B) detection using CF nanocubes as peroxidase mimic. Inset: The linear calibration plots for H_2O_2 (A) and glucose (B) determination. The error bars represent the standard deviation of the three measurements.

characteristic absorption peak of oxidized TMB. Meanwhile, the corresponding photograph of TMB solutions under different conditions is revealed in inset of Fig. S2. The color of TMB solution changed to deep blue only in the presence of both CF nanocubes and H_2O_2. All these observations suggest that the CF nanocubes can effectively catalyze the oxidation of TMB by H_2O_2 as peroxidase mimetics. Moreover, the absorption of TMB solution with CF nanocubes as catalyst is higher than those of PB, PBA and Fe_3O_4 (obtained by calcining PB precursor) (Fig. 4A). Although PB, PBA, Fe_3O_4 and CF nanocubes all can catalyze H_2O_2 to oxidate TMB, CF nanocubes exhibit the best catalytic performance as peroxidase mimetics. Thus, we assumed that the better catalytic performance of CF nanocubes may be mainly attributed to the hierarchical nanostructures[18] and the synergistic effect of Co and Fe element.[11, 30].

In order to establish the optimum analytical conditions, we measured the peroxidase-like activity of CF nanocubes, while varying the pH from 2 to 12 (Fig. 4B), the temperature from 20 to 70 ^oC (Fig. 4C), and the concentration of H_2O_2 from 1 to 1000 mM (Fig. 4D). Meanwhile, we compared the results with the activity found in HRP over the same range of parameters (Fig. 4). When the pH and temperature are approximately 4.0 and 40 ^oC, the CF nanocubes show the best catalytic performance, which are very similar to the values for HRP. But the CF nanocubes catalyzed reaction is inhibited at a higher concentration of H_2O_2 to reach the maximum level of peroxidase activity than that of HRP (Fig. 4D). The reusability of CF nanocubes was also evaluated on catalytic oxidation of TMB. Fig. S3 shows that ~85% of the initial catalytic activity of CF nanocubes was retained throughout 10 cycles.

A colorimetric method for detection of H_2O_2 was developed on the basis of the intrinsic peroxidase activity of CF nanocubes. As a result of the oxidized TMB is in proportion to the H_2O_2 concentration, H_2O_2 can be simply detected by using UV-Vis spectroscopy. Fig. 5A represents the H_2O_2 concentration-absorbance curves under optimal conditions. The linear range (inset in Fig. 5A) of H_2O_2 from 1 μM to 60 μM (R=0.9929) was obtained, with a detection limit of 0.36 μM. H_2O_2 is the main product of glucose oxidation by GOx in the presence of oxygen. Consequently, glucose detection could be realized by coupling CF nanocubes based catalytic methods with the GOx based glucose oxidation. The glucose concentration–absorbance curve at 652 nm is presented in Fig. 5B. From the calibration curve (inset in Fig. 5B), the linear range of glucose from 8 μM to 90 μM is realized (R=0.9898). The detection limit is estimated to be 2.47 μM at a signal-to-noise ratio of 3, which is lower than those of Fe_3O_4 nanoparticles (0.3 mM) [13] and LDH nanoparticles (0.4 mM) [31] based systems.

In order to evaluate the specificity of this glucose nanosensor, the interferences of common disaccharides (fructose, lactose and maltose) were investigated (Fig. S4A). Even when the concentration of control samples was 10 times larger than glucose, the absorbance of glucose was much higher than those of control samples. Thus, the colorimetric method is appropriate for the selective colorimetric detection of glucose. To examine the availability of the present method based on the enzyme-like CF nanocubes, we considered to detect glucose in human serum samples (Fig. S4B). According to the final absorbance and the calibration curve of glucose, the concentrations of glucose in three samples are calculated to be 5.80 mM, 9.62 mM and 9.48 mM with the relative standard deviation of 5.35%, 7.03% and 3.99%, respectively. The measured results are close to the reference value provided by the hospital (5.7 mM, 10.1 mM, 9.1 mM), which indicates this method is reliable in the determination of glucose in serum samples.

Conclusion

In summary, a new method using PB as precursor to synthesize hierarchical CF nanocubes was designed and developed. The CF hierarchical nanocubes were generated by water bath reaction of PB nanocubes with $CoCl_2$, followed by annealing the corresponding PBA precursor at 350 ^oC. The potential of CF nanocubes as a stable and effective peroxidase-like catalyst for the colorimetric detection of H_2O_2 was studied. The catalytic activity was dependent on temperature, pH, and H_2O_2 concentration. Subsequently, a convenient CF nanocubes based colorimetric assay was developed for detection of glucose. These excellent properties make the material a promising candidate for biomedical and biotechnology applications.

Notes and references

[a]State Key Laboratory of Electroanalytical Chemistry, Changchun Institute of Applied Chemistry, Chinese Academy of Sciences, Changchun 130022, (P. R. China)
Fax: +86 431-85262430; Tel: +86 431-85262430 ; E-mail: blzhang@ciac.ac.cn
Fax: +86 431-85262734; Tel: +86 431-85262734 ; E-mail: jltang@ciac.ac.cn
[b]University of Chinese Academy of Sciences, Beijing 100039 (P.R. China)

1. G. S. Lai, H. L. Zhang, T. Tamanna and A. M. Yu, *Anal Chem*, 2014, 86, 1789.
2. Y. J. Jiang, W. Tang, J. Gao, L. Y. Zhou and Y. He, *Enzyme Microb Technol*, 2014, 55, 1.
3. W. Wang, X. Jiang and K. Chen, *Chem Commun*, 2012, 48, 7289.
4. Y. Tao, Y. Lin, Z. Huang, J. Ren and X. Qu, *Adv Mater*, 2013, 25, 2594.
5. Y. Jv, B. X. Li and R. Cao, *Chem Commun*, 2010, 46, 8017.
6. Y. J. Song, K. G. Qu, C. Zhao, J. S. Ren and X. G. Qu, *Adv Mater*, 2010, 22, 2206.
7. J. Xie, H. Cao, H. Jiang, Y. Chen, W. Shi, H. Zheng and Y. Huang, *Anal Chim Acta*, 2013, 796, 92.
8. Z. Zhang, J. Hao, W. Yang, B. Lu, X. Ke, B. Zhang and J. Tang, *Acs Appl Mater Interfaces*, 2013, 5, 3809.
9. S. Dutta, S. Sarkar, C. Ray and T. Pal, *Rsc Adv*, 2013, 3, 21475.
10. Y. J. Yao, Z. H. Yang, D. W. Zhang, W. C. Peng, H. Q. Sun and S. B. Wang, *Ind Eng Chem Res*, 2012, 51, 6044.
11. X. Y. Niu, Y. Y. Xu, Y. L. Dong, L. Y. Qi, S. D. Qi, H. L. Chen and X. G. Chen, *J Alloy Compd*, 2014, 587, 74.
12. L. Q. Luo, Y. T. Zhang, F. Li, X. J. Si, Y. P. Ding, D. M. Deng and T. L. Wang, *Anal Chim Acta*, 2013, 788, 46.
13. H. Wei and E. Wang, *Anal Chem*, 2008, 80, 2250.
14. S. G. Christoskova, M. Stoyanova and M. Georgieva, *Appl Catal A-Gen*, 2001, 208, 235.
15. K. J. Kim, H. K. Kim, Y. R. Park, G. Y. Ahn, C. S. Kim and J. Y. Park, *Hyperfine Interact*, 2006, 169, 1363.
16. W. Shi, X. Zhang, S. He and Y. Huang, *Chem Commun*, 2011, 47, 10785.
17. Y. Fan and Y. Huang, *Analyst*, 2012, 137, 1225.
18. X. Liu, Z. Chang, L. Luo, T. Xu, X. Lei, J. Liu and X. Sun, *Chem Mater*, 2014, 26, 1889.
19. Q. Yang, Z. Lu, J. Liu, X. Lei, Z. Chang, L. Luo and X. Sun, *Prog Nat Sci*, 2013, 23, 351.
20. S. Chen and S.-Z. Qiao, *Acs Nano*, 2013, 7, 10190.
21. C. Ray, S. Dutta, S. Sarkar, R. Sahoo, A. Roy and T. Pal, *J Mater Chem B*, 2014, DOI: 10.1039/C4TB00968A.
22. Z. Zhang, Y. Wang, M. Zhang, Q. Tan, X. Lv, Z. Zhong and F. Su, *J Mater Chem A*, 2013, 1, 7444.
23. A. Biabani-Ravandi, M. Rezaei and Z. Fattah, *Process Saf Environ*, 2013, 91, 489.
24. Y. Fan, W. Shi, X. Zhang and Y. Huang, *J Mater Chem A*, 2014, 2, 2482.
25. Z. G. Jia, D. P. Ren and R. S. Zhu, *Mater Lett*, 2012, 66, 128.
26. J. C. Fu, J. L. Zhang, Y. Peng, J. G. Zhao, G. G. Tan, N. J. Mellors, E. Q. Xie and W. H. Han, *Nanoscale*, 2012, 4, 3932.
27. L. Zhang, H. B. Wu and X. W. Lou, *J Am Chem Soc*, 2013, 135, 10664.
28. J. H. Hao, W. S. Yang, Z. Zhang, S. H. Pan, B. P. Lu, X. Ke, B. L. Zhang and J. L. Tang, *Nanoscale*, 2013, 5, 3078.
29. J. Zhao, Y. Xie, W. Yuan, D. Li, S. Liu, B. Zheng and W. Hou, *J Mater Chem B*, 2013, 1, 1263.
30. J. Sun, Y. Li, X. Liu, Q. Yang, J. Liu, X. Sun, D. G. Evans and X. Duan, *Chem Commun*, 2012, 48, 3379.
31. Y. Zhang, J. Tian, S. Liu, L. Wang, X. Qin, W. Lu, G. Chang, Y. Luo, A. M. Asiri, A. O. Al-Youbi and X. Sun, *Analyst*, 2012, 137, 1325.